Journal of Marine Systems 78 (2009) 460–475

Contents lists available at ScienceDirect

Journal of Marine Systems

journal homepage: www.elsevier.com/locate/jmarsys

A conceptual model of the strongly tidal Columbia River plume

Alexander R. Horner-Devine [a,*], David A. Jay [b], Philip M. Orton [c], Emily Y. Spahn [a]

[a] Civil and Environmental Engineering, University of Washington, Seattle, WA, USA
[b] Civil and Environmental Engineering, Portland State University, Portland, OR, USA
[c] Lamont-Doherty Earth Observatory, Columbia University, Palisades, NY, USA

ARTICLE INFO

Article history:
Received 8 November 2006
Received in revised form 2 June 2008
Accepted 10 November 2008
Available online 20 February 2009

Keywords:
River plume
Fronts
Tides
Residence time
Internal waves
Columbia River

ABSTRACT

The Columbia River plume is typical of large-scale, high discharge, mid-latitude plumes. In the absence of strong upwelling winds, freshwater from the river executes a rightward turn and forms an anticyclonic bulge before moving north along the Washington coast. In addition to the above dynamics, however, the river plume outflow is subject to large tides, which modify the structure of the plume in the region near the river mouth. Observations based on data acquired during a summer 2005 cruise indicate that the plume consists of four distinct water masses; source water at the lift-off point, and the tidal, re-circulating and far-field plumes. In contrast to most plume models that describe the discharge of low-salinity estuary water into ambient high-salinity coastal water, we describe the Columbia plume as the superposition of these four plume types. We focus primarily on a conceptual summary of the dynamics and mutual interaction of the tidal and re-circulating plumes. The new tidal plume flows over top of the re-circulating plume and is typically bounded by strong fronts. Soon after the end of ebb tide, it covers roughly 50–100% of the re-circulating plume surface area. The fronts may penetrate well below the re-circulating plume water and eventually spawn internal waves that mix the re-circulating plume further. The re-circulating plume persists throughout the tidal cycle and corresponds to a freshwater volume equivalent to 3–4 days of river discharge. Finally, the plume water masses are distinguished from one another in term of surface chlorophyll concentration, suggesting that the above classification may also describe different biological growth regimes. The low-salinity re-circulating plume serves as an extension of the estuary into the coastal ocean, or an "estuary at sea", because residence times during periods of high river flow are greater than those in the estuary.

1. Introduction

The Northwest shelf of the United States is subject to moderately strong tidal forcing, with amplitudes of 2 to 4 m at the mouth of the Columbia River estuary. The tides, focused by a long estuary channel, cause reversing estuarine outflow velocities of 1 to 3 ms^{-1} and a pulsed discharge from the estuary to the shelf. While recent numerical model experiments do not report a significant change in the structure of the far-field plume when the river outflow is modulated on tidal timescales (Yankovsky et al., 2001), observations of the Columbia plume suggest that the region within approximately 50 km of the river mouth is complex, with characteristics that vary over relatively small spatial and temporal timescales as a result of this periodic forcing. Outgoing tidal pulses overrun existing plume water, generating intense fronts and extensive bands of internal waves that mix the new plume, old plume and ambient coastal water. The dynamics of this region determine the initial exchange of nutrients between the plume and ocean waters and set the stage for a highly productive coastal ecosystem.

River plume fronts have been the subject of a number of observational and analytical studies (Garvine and Monk, 1974; Garvine, 1974; O'Donnell et al., 1998; Orton and Jay, 2005). The front is defined as the narrow region on the water surface where the density changes rapidly, forming a boundary between the outward propagating lens of buoyant water and the ambient receiving water (Garvine and Monk, 1974; Garvine, 1974). Propagation perpendicular to the front leads to convergence at the front and forces ambient water and buoyant water downwards (O'Donnell et al., 1998). Pritchard and Huntley (2006) compare the interfacial mixing at a plume front with the total buoyancy input from the estuary to determine the conditions leading to plume formation and destruction. For the small-scale River plume in the English Channel, the buoyancy flux from the estuary initially exceeds frontal mixing, which is the dominant mixing mechanism in the absence of strong winds. Over the course of the tidal cycle, frontal mixing surpasses the buoyancy flux and eventually disperses the plume. In large-scale plume and oceanic fronts, the outward propagation of the front is limited by the earth's rotation (Garvine, 1979a,b). The scale of these fronts is characterized by the baroclinic Rossby radius, and they develop strong front-parallel shear.

The role of tides in the dynamics of coastal plumes has been the subject of several numerical model studies. Chao (1990) showed that

* Corresponding author.
E-mail address: arhd@u.washington.edu (A.R. Horner-Devine).

0924-7963/$ – see front matter © 2009 Elsevier B.V. All rights reserved.
doi:10.1016/j.jmarsys.2008.11.025

tidal modulation contributes a subtidal vortex dipole, akin to that described by Zimmerman (1981), to the existing outflow circulation, which slightly increases the cross-shore expansion of the plume in the region near the mouth and decreases the alongshore penetration of the coastal current. In a more recent numerical model study, Yankovsky et al. (2001) reported very little difference between the structure of a plume subjected to semidiurnal tidal fluctuations and that of a non-tidal plume. Due to numerical model constraints, neither study captures changes in the small-scale dynamics or mixing of the plume that may result from tidal fluctuations. As noted above, these are likely to be important in determining how the plume affects the local coastal ecosystem.

In this work we develop a conceptual model that describes the plume water masses in the region near the river mouth. We initially ignore the effect of wind stress in order to examine the more basic plume dynamics. The effect of wind is discussed as an extension of the conceptual model and a more thorough description is presented in a companion paper Jay et al. (this volume), referred to as DJ. We outline the conceptual model in terms of scales that define the different components of the plume. We then present results from observations of the Columbia plume during a low-wind period in 2005, when the components of the plume can be differentiated. Finally, we synthesize the results to suggest the role that the tidal plume front plays as the components of the plume interact, and the ecological importance of the re-circulating plume as an extension of the estuary into the coastal ocean.

2. Conceptual model

2.1. Physical setting

The Columbia River flows into the Pacific Ocean near Astoria, Oregon on the border between Oregon and Washington states (Figs. 1 and 2). It is among the four largest rivers entering the ocean in the United States with an annual mean discharge of approximately 7300 $m^3 s^{-1}$ (Barnes et al., 1972; Hickey et al., 1998). The tidal range in the vicinity of the mouth is large and the main estuary channels are relatively narrow (1–2 km), resulting in a salinity intrusion that propagates 5 to 50 km upstream from the mouth. The river mouth is 3 km wide and oriented towards the south west. As a result of complex bathymetry in the estuary channel near the mouth, the estuarine outflow discharges approximately due west during maximum ebb. The shelf off of Oregon and Washington slopes steeply away from the coast, resulting in a plume that detaches from the bottom close to the river mouth. Garvine (1995) developed a classification for river plumes based on the observed plume scales. Plumes with high Kelvin number, defined as $K = fW_p(g'_p H_p)^{-1/2}$, are considered to be large scale plumes and are characterized by linear dynamics and a cross-shore geostrophic balance. Here W_p, g'_p, and H_p are representative scales for the plume width, reduced gravity and depth. For the Columbia, $W_p = 20$ km, $H_p = 10$ m and $g'_p = 0.1$ m s^{-1}, and thus $K = 2$. This is a relatively large value of K, according to the Garvine (1995) classification, and suggests that the Columbia be considered a large-scale plume. Such a classification is consistent with regional scale field studies of the plume (Hickey et al., 1998).

In a relatively large region near the mouth, however, high river discharge and large tidal amplitude result in strongly non-linear dynamics. Based on the average annual flow, river width $W = 3$ km, an approximate layer depth of $H = 5$ m and reduced gravity $g' = \Delta\rho\rho_o^{-1} = 0.21$ m s^{-2}, the internal Froude number of the outflow is $Fr = U(g'H)^{-1/2} = 0.5$, where $U = 0.5$ m s^{-1} is the mean outflow velocity, $\Delta\rho$ is the density anomaly and ρ_o is the reference density. The inflow Rossby number for the same parameters is $Ro = U(fW)^{-1} = 1.6$, where f is the Coriolis frequency. During peak ebb, the estuary discharge may be more than four times the river discharge and the outflow velocity exceeds 3 m s^{-1}. Under these conditions, $Fr = 2.0$ and $Ro = 6.4$. These values suggest a jet-like outflow that is dominated by the momentum of the river close to the mouth; the Coriolis force only becomes important once the plume has expanded and slowed away from the mouth. The supercritical Fr implies that the outflow will develop strong, convergent density fronts in the region offshore from the river mouth. These dynamics are more commonly associated with small-scale river plumes such as the Connecticut or Teign rivers (Garvine, 1995; O'Donnell et al., 1998; Pritchard and Huntley, 2006). In small-scale plumes, however, the river discharge is much smaller than that of the Columbia and their impact on the coastal hydrography is correspondingly smaller. In addition, the new plume that is discharged with each ebb generally propagates into high salinity coastal water and is significantly dissipated by the time of the following ebb. As demonstrated in the current work, this is often not the case for the Columbia plume. The combination of a high-discharge, large-scale plume with a supercritical tidal plume leads to complex dynamics. The aim of the present conceptual model is to describe the plume in terms of its components so that the dynamics can be better understood.

2.2. Plume anatomy

We propose a conceptual model, in which the Columbia plume is described in terms of four water masses: source water, the tidal plume, the re-circulating plume and the far-field plume. A cartoon of the four water masses for the low-wind case is shown in Fig. 3a. Water originating in the river moves sequentially through the source zone, which is close to the river mouth, and then into the tidal plume as it is discharged onto the shelf. Depending on wind conditions, it may be retained in the re-circulating plume before it becomes far-field plume water and is subsequently mixed into the ambient shelf water. Although these water masses are associated with different physical regions of the plume (Fig. 3a), they are also differentiated in terms of their respective time scales and salinity due to the large variability in the plume structure. It is natural to define the plume components based on salinity bounds since they correspond roughly to progressive stages in the mixing of river water into the ocean. However, the salinity thresholds that differentiate between different plume components will vary depending on the intensity of mixing processes, which are modified by tides, winds and river discharge. For example, the salinities that characterize the tidal plume will likely be lower during a neap tide in high discharge conditions than during a spring tide in low discharge conditions due to the high vertical density stratification and relatively lower energy available for mixing in the former case. In the following description of the plume components a salinity range is proposed for each that corresponds to the conditions observed during surveys in the first week of June 2005. They are representative of moderately high discharge conditions close to the spring tide and are justified in more detail in Section 4.1. Analysis of how different conditions modify the salinity range is left for future work.

The two remote sensing images of the plume shown in Fig. 2a and b illustrate different components of the plume structure in low-wind conditions. In the SAR image (Fig. 2a) lighter shading corresponds to high backscatter, indicating regions of enhanced surface roughness (Hessner et al., 2001). In the Columbia plume, bands of high SAR backscatter occur in association with strong fronts and internal waves. The image is taken 10.5 h after high tide on June 3, 2005 and shows the semi-circular tidal plume front, which is roughly symmetric about the river mouth. At the time of the image, the front extends approximately 36 km from the river mouth. It is strong to the north of the mouth and has dissipated south of the mouth. A series of solitons have been released from the western edge of the front; these are released earlier on the south than the north based on the spacing between the waves (DJ).

In the MODIS image from May 16, 2006 (Fig. 2b), lighter colored pixels correspond to greater concentrations of suspended matter near the water surface. This image shows the rough delineation of the complete plume. Near the river mouth, water discharged from the

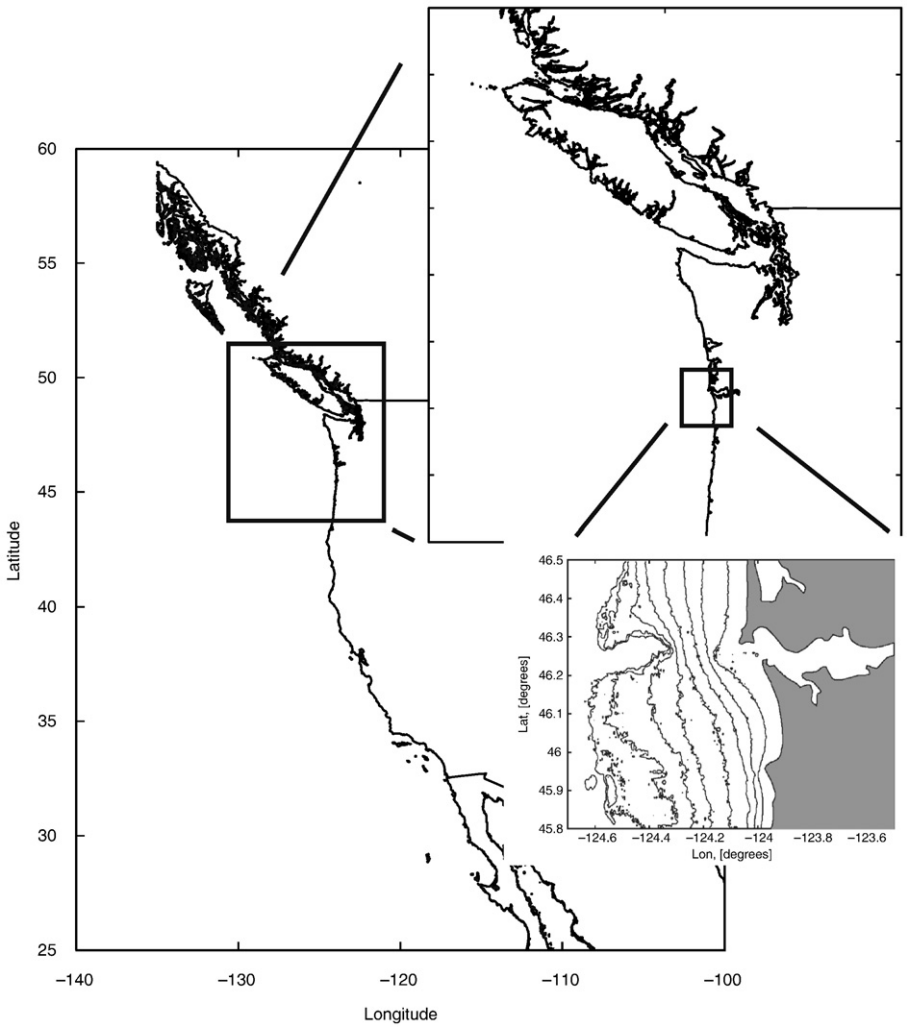

Fig. 1. Location of the mouth of the Columbia River and study site.

estuary forms a large bulge extending 22 km offshore. North of the bulge, the plume water moves northward in a coastal current. According to the conceptual model presented here, the bulge consists of the re-circulating plume, over which the tidal plume periodically pulses. The remainder of the plume extending north along the coast and, to a lesser degree, south and offshore, is considered the far-field plume. Note that the two images are taken at different times of year and under different forcing conditions.

2.2.1. Source water

The plume source region is the area at the entrance of the estuary where low-salinity estuarine water loses contact with the seabed to form the nascent plume. The actual plume lift-off position is a function of river flow and tidal range. Thus, the source zone, functionally defined as the waters between the most-landward and most-seaward lift-off points, has a finite extent. For currently observed river flow levels, plume lift-off occurs 3 to 7 km from the ocean. It roughly coincides with the location of a lateral constriction formed by a stone jetty 5 km from the ocean, which acts as an internal hydraulic control (Cudaback and Jay, 2000). The source water transits through the source zone in approximately 2 h and typically has salinity less than 12. It is estuarine surface water that has undergone mixing at the time of lift-off with higher salinity water (MacDonald and Geyer, 2004). Although a significant portion of the plume dilution occurs in the source region, it is not accessible with our sampling platform. Our discussion, therefore, focuses on the three offshore components of the plume: the tidal, re-circulating and far-field plumes.

2.2.2. Tidal plume

The tidal plume is the pulse of estuary water discharged onto the shelf during the ebb tide. It is energetic, strongly stratified, and typically bounded on its outer edge by sharp fronts. For the time period that we consider, the salinity of the water in the tidal plume is below 21 and its associated time scale is 6–12 h. The tidal excursion L_T based on an average estuarine outflow velocity of 1 m s^{-1} is approximately 20 km, which is representative of the initial propagation of the tidal plume. As the SAR image in Fig. 2a and our observations suggest, however, the tidal plume propagates away from the mouth well after the tide reverses and is characterized by horizontal scales on the order of 35 km. The combined river and tidal outflow from the estuary is approximately 6×10^8 m^3. Assuming that the majority of the mixing has occurred in the source region and that the tidal outflow diverges laterally at an angle of approximately 30°, the average depth of the tidal plume is approximately 6 m at the end of the ebb and less than 3 m at its greatest lateral extent. It is clear from the SAR image in Fig. 2a that the tidal plume forms a semi-circular front. Thus, the spreading angle assumed above may not represent the entire lateral extent of the tidal plume and, our estimates of the plume depth are likely to be high. In its initial propagation away from the river mouth the tidal plume is supercritical and its dynamics are dominated by the inertia of the estuary discharge. For the purposes

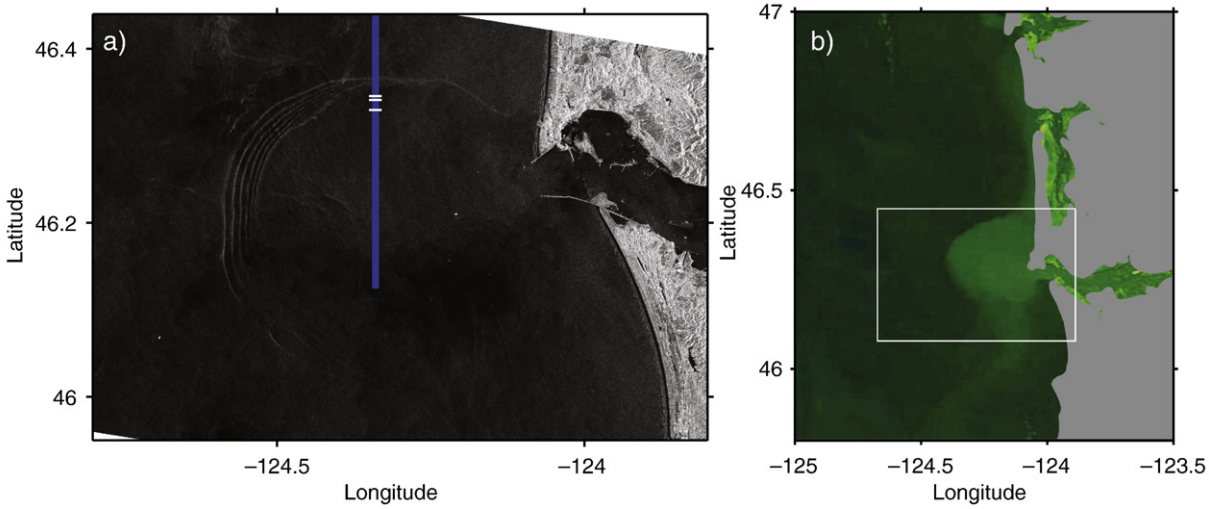

Fig. 2. Remote imagery of the Columbia River plume. a) SAR image taken 10.5 h after high tide on June 3, 2005. The semi-circular front and five solitons (outside the front) are evident as light colored lines in the image, which is sensitive to changes in surface roughness. The ship track for sampling on June 10, 2005 is shown in blue and the location of consecutive front crossings on that day is shown as white hatches on the transect line. b) True color image from the MODIS Terra sensor taken 5.5 h after high tide on May 16, 2006. The image has been enhanced so that variability in the plume contrast is greater. The rectangle coincides with the region shown in a). Image courtesy of Raphael Kudela, UCSC. (For interpretation of the references to colour in this figure legend, the reader is referred to the web version of this article.)

of the conceptual model, therefore, we will assume wind and the earth's rotation play a minor role in the evolution and scales of the tidal plume.

2.2.3. Re-circulating plume

The re-circulating plume consists of water that has been on the shelf between 0.5 and 4 days and corresponds to the bulge region observed in laboratory and numerical model experiments. In this region, plume water is strongly affected by the earth's rotation as well as the momentum of the river discharge. The salinity in the re-circulating plume is between 21 and 26. The scale of the re-circulating plume may be estimated based on laboratory experiments. The cross-shore displacement of the bulge in laboratory experiments has been shown to scale with the inertial radius, $L_i = Uf^{-1}$ (Horner-Devine et al., 2006). For typical values of the Columbia plume during ebb tide, $L_i = 10$ km. In the laboratory experiments, the bulge radius is $2L_i$ after 3 to 4 days, and continues to grow indefinitely. Thus, the cross-shore extent of the re-circulating plume is expected to be approximately 40 km after 3 to 4 days. For the purposes of the present discussion, we will designate a scale L_B as the cross-shore width of the plume in the vicinity of the river mouth. According to laboratory studies L_B scales with L_i when there is negligible wind stress. The effect of local winds on plume scales will be discussed in Section 5.

2.2.4. Far-field plume

The far-field plume is the zone beyond the re-circulating plume where final mixing of plume and ambient seawater occurs. It is driven

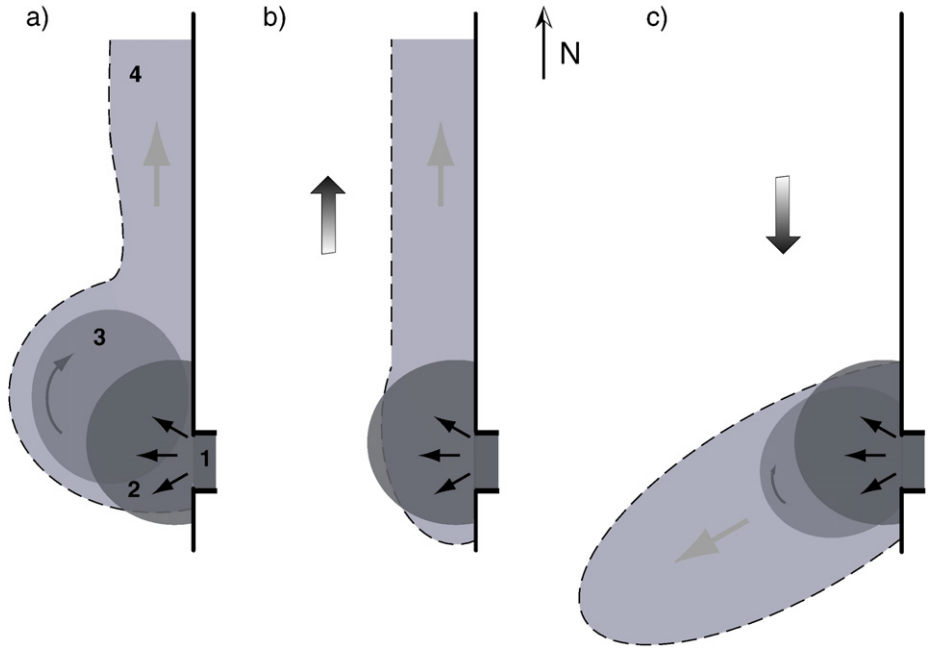

Fig. 3. Conceptual model of the Columbia River plume under three wind forcing conditions. a) Plume with low wind forcing showing four water masses: source (1), tidal (2), re-circulating (3) and far-field (4). b) Plume during a period of sustained downwelling wind, which compresses the re-circulating and far-field plumes against the coast resulting in a tidal plume that extends further offshore than the rest of the plume. c) Plume during a period of sustained upwelling wind. In this case the near-surface Ekman flux draws the re-circulating and far-field plumes offshore and the tidal plume propagates primarily into stratified plume water.

by buoyancy, the earth's rotation, wind and ambient currents and is not directly affected by the momentum of the river discharge. The far-field plume is typically distinguished from ambient ocean water based on a threshold salinity of 32.5. Time scales for retention of fluid in the far-field plume depend on external conditions such as wind and are probably in the range 2 to 10 days. The far-field plume generated by the Columbia River has been observed to extend as far north as the Straits of Juan de Fuca and seaward of the continental shelf. Its growth appears to be limited primarily by the time between storm events that mix the plume into the ambient coastal waters and its volume is related to recent river discharge history.

The above classification modifies that of Garvine (1982), who divides the plume into source, near-field and far-field regions. The near-field described by Garvine (1982) is the region where the initial expansion of the plume occurs and is bounded by strong fronts. Our classification is very similar to that of Garvine (1982), except that it decomposes the near-field plume into the pulsed tidal plume and the residual re-circulating plume. Thus, the re-circulating plume is an intermediary water mass between the tidal and far-field plumes.

2.3. Interactions between plume water masses

Differentiation between the tidal and re-circulating plumes is useful for describing the interaction between these two water masses, which is important in the initial propagation and mixing of the plume. The tidal plume propagates directly into and over the re-circulating plume, from which it is typically separated horizontally by a strong front. Orton and Jay (2005) observe eddy diffusivities O ($0.2\ m^2\ s^{-1}$) 50 m behind the front, and estimate that frontal mixing accounts for 20% of the salt flux into the tidal plume. Nash and Moum (2005) describe solitons that are released from the tidal plume front, which may result in further mixing. While the frontal mixing will exchange new tidal plume water with older plume water, the solitons propagate away from the tidal plume through older plume water and primarily mix older plume water with ambient water masses. The re-circulating plume receives buoyant water from the tidal plume as described above and incorporates it into a less energetic, gyre-like circulation that persists beyond the tidal time scale.

Without winds, the length scale of the tidal plume L_T is approximately equal to the length scale of the re-circulating plume, L_B, and the two are closely coupled. The propagation speed, mixing and soliton formation of the tidal plume all depend on the stratification of the re-circulating plume water into which the tidal plume flows. The spreading of the tidal plume transfers energy, momentum and buoyancy to the re-circulating plume. Ultimately, the tidal water losses its initial momentum and melds into the re-circulating plume, thereby setting the conditions for the subsequent ebb pulse. In the absence of the re-circulating plume, the residence time of low-salinity water in the vicinity of the river mouth is greatly decreased, and subsequent tidal plumes propagate instead into ambient, higher-salinity coastal water.

The model presented above describes the low-wind case. However, it is easily extended to describe the expected plume behaviour in upwelling and downwelling conditions. In these conditions the wind strongly modifies the structure of the re-circulating and far-field plumes (Garcia-Berdeal et al., 2002), while the structure tidal plume is relatively less affected. This is discussed in Section 5 and observations of the plume under these conditions are presented in DJ.

3. Description of study

3.1. The RISE project

The proposed conceptual model is based on observations of the Columbia River plume during the River Influences on Shelf Ecosystems (RISE) project. The overarching goal of the project is to understand the role of the Columbia plume in the marine ecosystem along the Oregon and Washington shelf. To address this complex question, each cruise consisted of two vessels, the R/V Pt Sur and the R/V Wecoma, which made a multitude of biological, geochemical and physical process measurements. Despite its large size and persistent presence on the northwest shelf, the Columbia plume is difficult to sample because it is very shallow and transient, with complex and relatively small-scale spatial variability that changes over short timescales (Garcia-Berdeal et al., 2002; Hickey et al., 2005). The proposed conceptual model is intended to provide a framework for interpreting the possible states of the plume.

RISE sampling spanned three years and included four 3–4 week long cruises: July 2004, June 2005, August 2005 and June 2006. During these field campaigns, the Columbia River plume was observed under a variety of forcing conditions including annual changes in coastal conditions, seasonal changes in river discharge, spring–neap tidal variability and daily changes in meteorological forcing. The sampling strategy was organized in such a way that both the large-scale and small-scale structures of the plume could be observed. It included regional mapping studies, which spanned three to four days and covered scales on the order of 50 to 100 km, process studies, which typically repeated 10 to 30 km sections, and stationary time series.

3.2. Instrumentation

Sampling river plumes is challenging since they are transient, wide, thin and surface-trapped. The vertical sampling resolution must be at least 10 cm, the horizontal sampling range must be on the order of 10 km and the sampling interval must be sufficiently short to avoid tidal aliasing. In order to sample the near-surface water column (0–30 m depth) at sufficient horizontal speeds, instruments were mounted on a TRIAXUS tow fish. The TRIAXUS is a towed platform, steerable in 3D, so that surface waters can be sampled outside the vessel wake. The TRIAXUS sampled to within 1 m in smooth conditions and 2–3 m in rougher conditions. The TRIAXUS was fitted with three CTDs, an upward-looking ADCP, a laser particle sizer (LISST-FLOC), and a Laser Optical Planktoncounter. This study focuses primarily on data collected with the Seabird CTD and a downward-looking 1200 kHz ADCP that was pole-mounted to the side of the vessel near the water surface.

The TRIAXUS is a valuable platform for plume studies as it permits sampling close to the surface at relatively high vessel speeds. In the region surrounding the mouth of the Columbia River, however, the TRIAXUS was very susceptible to snags on crab pots, which often required lengthy repairs on deck. This occurred in the middle of the sampling program described herein, and resulted in the loss of CTD data for one fifth of the fourth transect and all of the fifth and sixth transects on Line B.

3.3. Sampling lines

We consider three sampling lines, which cross the region occupied by the tidal, re-circulating and far-field plumes. Line A runs diagonally across the estuary outflow and was occupied repeatedly throughout the study (Fig. 4). It is the shallowest inshore line that we were able to sample with the TRIAXUS. Line B runs 30 km north-south approximately 25 km west of the river mouth. Line C runs approximately 30 km directly west from a starting point 5–10 km from the mouth.

The low-wind scenario described in Section 2 was observed during sampling on June 8–10, 2005. A total of 16 transects on lines A and B captured the structure of the plume close to the mouth and further from shore through the middle of the re-circulating plume. Ten transects on Line A (referred to as transects A1–A10) were carried out starting at 0:00 h GMT on June 8 until 12:00 on June 9. Six transects on Line B (referred to as transects B1–B6) were carried out starting at 18:00 h on June 9 and until 12:00 on June 10. As occurred on a number

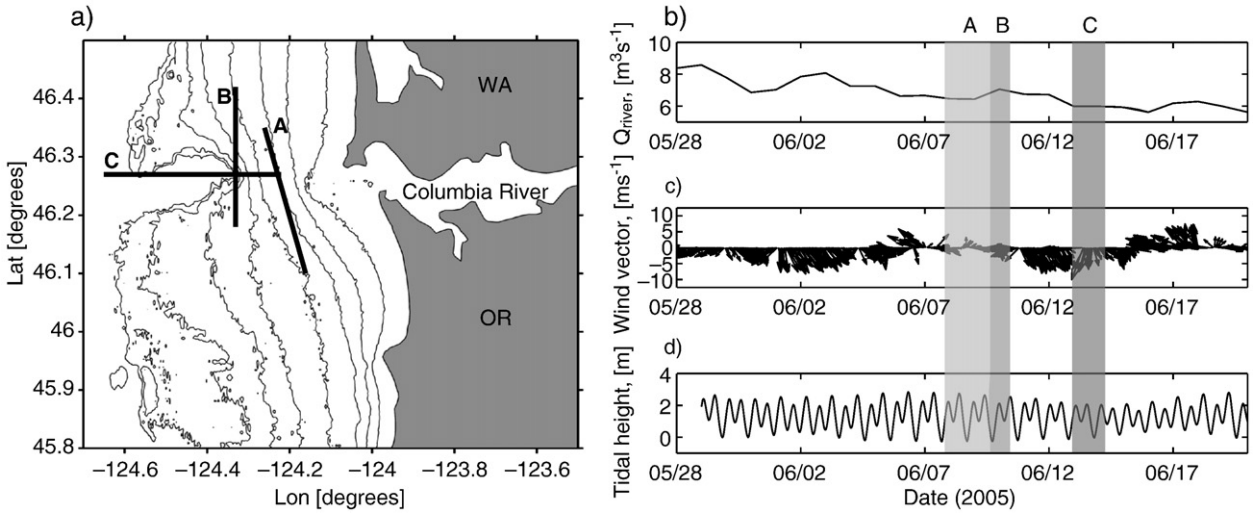

Fig. 4. a) Locations for the three transects of interest during the June 2005 cruise. b) Columbia River discharge measured by the USGS at the Beaver Army Terminal, Quincy OR. (c) North and East wind velocity components from NOAA buoy 46026 near the mouth of the Columbia River. The shaded bars correspond to periods during which transects A, B and C (shown in a), were occupied.

of occasions, the TRIAXUS snagged a crabpot during the fourth pass and was damaged. We continued to sample without the TRIAXUS, relying on the vessel's underway system for surface salinity in addition to ADCP data.

The cross-shore structure of the plume was sampled on Line C during a 25 h period two days later. During the period between sampling on Lines A/B and Line C the wind was persistent from the North with magnitude between 5 and 10 m s^{-1}. The persistence and strength of the wind appears to have been sufficient to set up the upwelling circulation. The wind and upwelling circulation were maintained over the period of sampling on Line C. Thus, the observations do not describe the same low-wind scenario observed during sampling of Lines A and B. It is evident, however, that the initial propagation of the tidal plume is not directly affected by the wind, and thus sampling on Line C documents the westward propagation of the tidal plume.

3.4. Conditions

The peak river discharge in the spring of 2005 occurred around May 20, 18 days prior to the sampling described here. On June 9 and 10, the average discharge was approximately 7000 m^3 s^{-1} (Fig. 4b). The sampling on Line B came at a time when the wind speed was moderate and the direction was variable (Fig. 4c). The winds did not generate persistent upwelling or downwelling conditions during this period. Prior to this period, the winds were predominantly from the North, resulting in sustained upwelling conditions for 5 to 7 days. Under such upwelling conditions, the plume is typically directed offshore and northward transport is low (Hickey et al., 2005). The observed plume behavior, therefore, appears to have commenced 3–4 days prior to the sampling period. Tides in the vicinity of the Columbia plume are mixed semidiurnal and have amplitudes in the range of 2 to 4 m. The sampling was four days after spring tide (Fig. 4d).

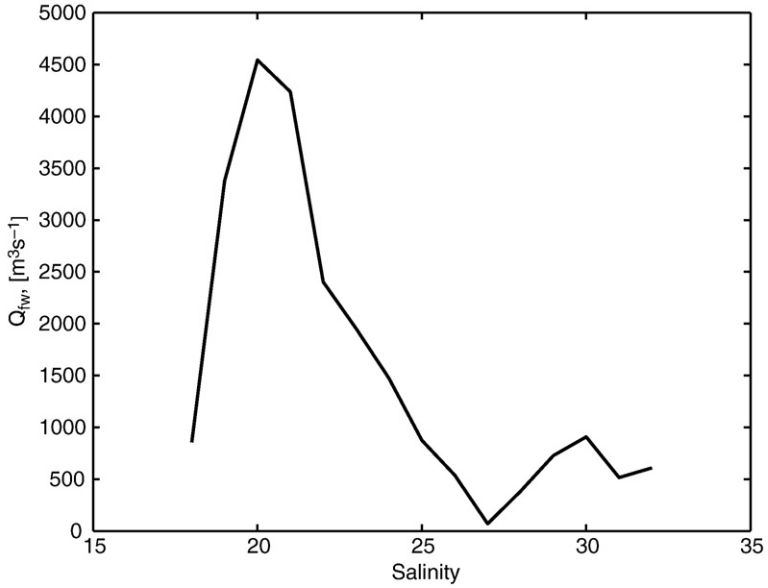

Fig. 5. Distribution of freshwater during the ebb tide on June 8, 2005 based on sampling on Line A. The flux was computed assuming a reference salinity of 27 for the coastal waters near the river mouth.

4. Results

The conceptual model introduced in Section 2 is based on observations of the plume during the four RISE cruises and intended to provide a framework for interpreting further observations of the plume. A primary goal of the model is to differentiate between the four water masses, which are characterized by different dynamics, responses to meteorological forcing and, potentially, biological dynamics. In this section data from transect lines A, B and C are presented that illustrate the three offshore water masses and their mutual interaction. First, the methodology for determining the salinity thresholds that we use to differentiate between water masses is presented. The observations of the tidal and re-circulating plumes are then described in detail as well as their modes of interaction. Finally, observations from line C are presented that briefly describe the constituents of the plume under upwelling conditions.

4.1. Delineation of plume water masses

It is convenient to describe the components of the plume with respect to salinity (Hetland, 2005). In practice, however, distinguishing between the tidal and re-circulating plumes based on salinity is challenging in the region close to the river mouth. We chose to define the maximum salinity of the tidal plume based on the salinity at which most of the horizontal freshwater flux was observed during peak ebb (Transect A5, Fig. 6). Here, the freshwater flux is calculated according to

$$Q_{fw} = \iint -u\frac{S_o - S}{S_o}dydz \tag{1}$$

where u is the east velocity component, S_o is the reference salinity, S is the salinity, and y and z are the north and vertical coordinates, respectively. The integration is carried out across the outflow section of the transect between 46.18° N and 46.30° N, and projected onto a vertical and north-south plane that is perpendicular to the outflow. Eq. (1) is sensitive to the choice of S_o, which represents the average salinity of the coastal water into which the tidal plume propagates. Choosing $S_o = 33$, consistent with a typical coastal salinity, greatly overestimates the freshwater flux, since it includes in the flux estimate lower salinity water from previous ebb tides that is entrained into the new tidal plume.

In order to determine the correct reference salinity, we sought the value of S_o that resulted in a total freshwater flux, averaged over the

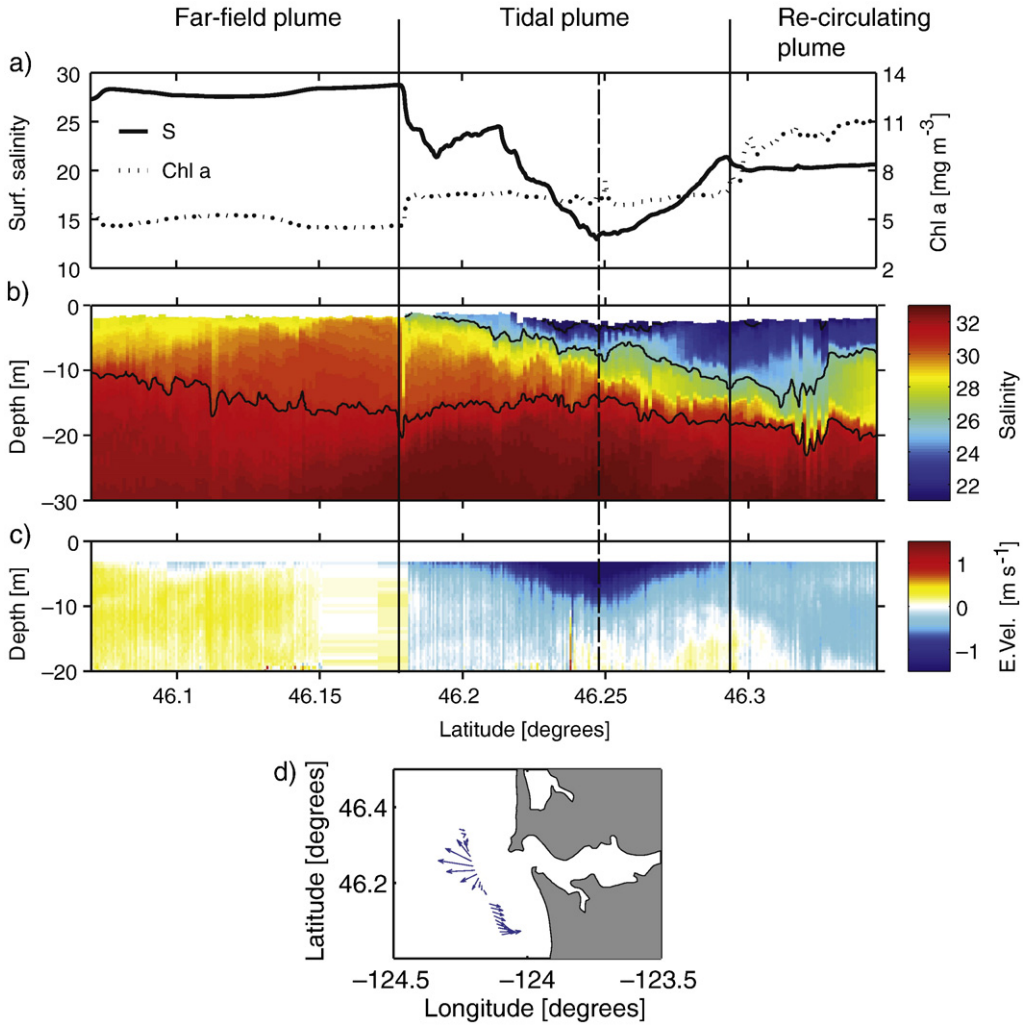

Fig. 6. Data from Line A5, 4.2 h after high tide on June 8, 2005. This transect intersects estuary outflow and the anticyclonic circulation, though the transect was cut short on this pass and the recirculation is not visible. a) Surface salinity (solid) and chlorophyll concentration (dot) from the vessel underway sampling system. b) Salinity from the TRIAXUS towfish in the upper water column. The black contours are 21, 26 and 32 salinity isohalines, which approximately delineate the tidal, re-circulating and far-field plume water masses. c) East velocity. d) Surface velocity vectors showing the strong, diverging estuary outflow. The solid vertical lines approximately delineate the three offshore water masses according to the surface salinity record. The dashed vertical line marks the approximate axis of the plume outflow.

entire 24.8 h tidal cycle, equal to the average river discharge during that period. The freshwater flux was calculated for each transect on Line A, interpolated to achieve hourly flux estimates across the entire tidal cycle, and averaged to get a daily estimate of the freshwater flux. The salinity for each cast in the transect was extrapolated to the water surface. We used a linear extrapolation for in-plume casts where there were sufficient data points to get a good fit, and assumed a constant surface salinity equal to the measured value closest to the water surface where such a fit was not achieved. This calculation was repeated with incrementally lower values of S_o until the computed daily average freshwater flux matched the daily average river discharge of 7000 $m^3 s^{-1}$ (Fig. 4b). Based on this method, the reference salinity was found to be $S_o = 27$.

Using the above value of S_o, the freshwater flux at each point in the outflow section of the ebb transect (Transect A5, Fig. 6) can be computed. When the freshwater flux is bin-averaged with respect to salinity, a distinct peak is observed for $S<21$, which accounts for 64% of the freshwater flux (Fig. 5). Note that the total freshwater flux of tidal plume water observed for transect A5 is approximately 25,000 $m^3 s^{-1}$, which greatly exceeds the average daily freshwater discharge. Based on this analysis, we define the upper salinity threshold of the tidal plume as $S = 21$. This choice is also guided by the observation that the northern front of the tidal plume occurs at a value of $S = 21$ as it is observed in the surface salinity record (Figs. 6a, 8a, 9a and 10a).

In Horner-Devine (2009), the salinity range $21 < S < 26$ corresponding to the re-circulating plume is defined based on the stratification at the base of the plume and comparison between the salinity and velocity in the re-circulating plume. The upper limit is lower than the reference salinity observed above, since the latter includes mixing of the tidal plume with higher salinity coastal water as well as re-circulating plume water. This is likely to occur, for example, on the southern edge of the tidal plume, where there is no re-circulating plume (Fig. 3a).

Finally, the far-field plume is defined as coastal water with salinity less than the ambient coastal water, $S<32.5$ (Barnes et al., 1972), but greater than the salinity in the re-circulating plume, $S>26$.

The three offshore plume water masses are delineated clearly in the record of surface salinity (Fig. 6a). South of 46.18° N, the surface salinity is very uniform and between 27 and 29. Although this is relatively close to the river mouth, the salinity indicates that this is far-field plume water. North of 46.29° N the salinity is also uniform and is slightly higher than 21. This is characteristic of the re-circulating plume and, according to the conceptual model, corresponds to water that was discharged from the estuary during a previous tidal cycle. Between these two uniform regions the surface salinity drops below 21, corresponding to the tidal plume water mass. The rapid salinity change on the south edge of the tidal plume indicates a strong front, which is also evident in the salinity data from the TRIAXUS and the velocity data (Fig. 6b and c). The front penetrates more than 20 m below the surface.

Transect A5 was cut short on this particular pass and does not extend north to capture the full extent of the plume. The re-circulating plume is clearer in Transect A7, which corresponds to a period 14 h

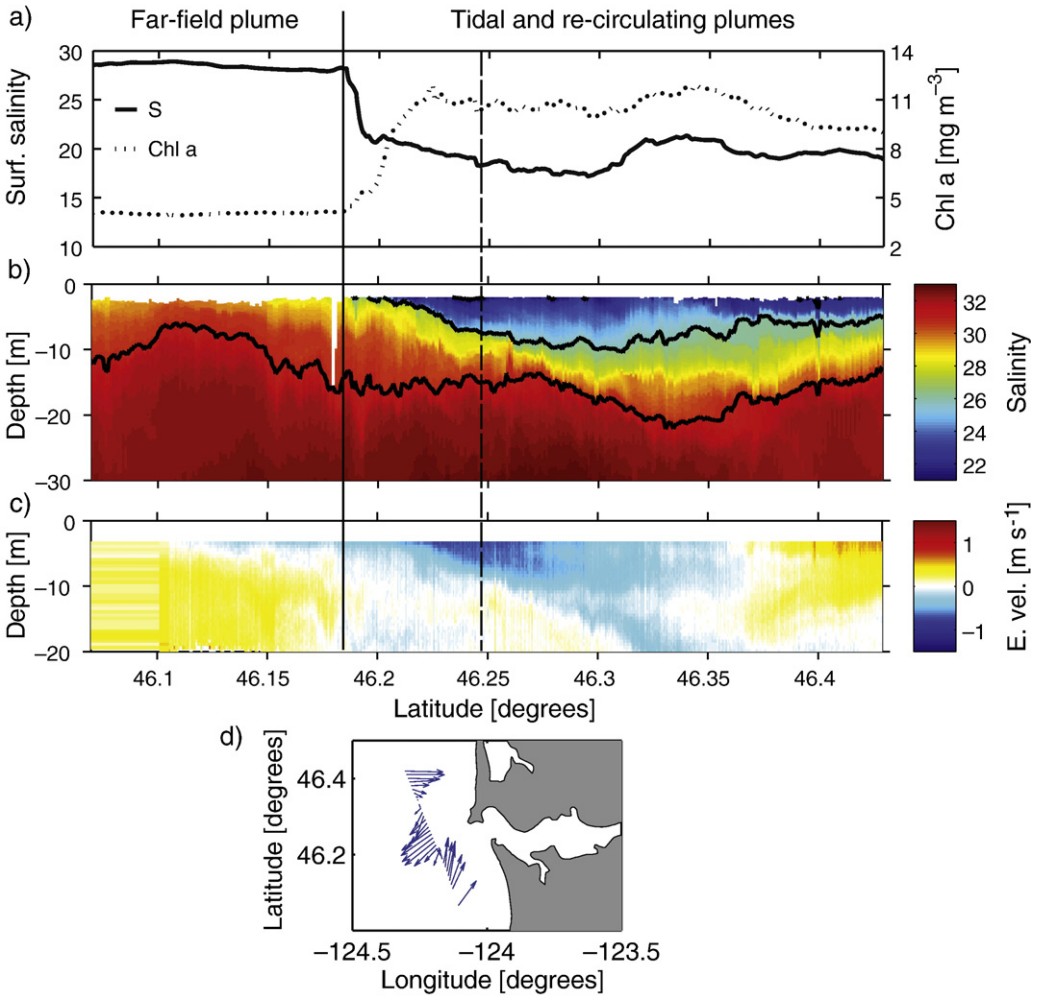

Fig. 7. Data from Line A7, 7.1 h after high tide on June 8, 2005. This transect intersects estuary outflow and clearly shows the anticyclonic circulation. See description of panels in Fig. 6 caption.

after the peak ebb (Fig. 7). The deeper isohalines outline a roughly bowl-shaped plume, with outgoing (westward flowing) water to the south and returning water to the north (Fig. 7b). Low-salinity water extends down to 20 m, but the active recirculation is limited to the upper 5 to 10 m of the water column (Fig. 7c).

4.2. Tidal plume

The tidal plume is initiated during the maximum ebb and propagates westward as a radially spreading jet that is approximately 5 km wide as it crosses transect line A (Fig. 6). The freshest water (<21) during the initiation of the tidal plume is limited to the top 3 m of the water column, while strong westward flow is observed down to 8 m depth (Fig. 6b and c). The surface velocity in the tidal plume is high, reaching a maximum of more than 3 m s^{-1} in the upper-most measurement bin. The lateral structure of the surface velocity field is consistent with the dipole model suggested by Chao (1990), with cyclonic vorticity south of the plume axis and anticyclonic vorticity north of the plume axis (Fig. 6e) Although the highest velocities tend northward, indicating Coriolis deflection in the center of the jet, the cyclonic and anticyclonic vorticity magnitudes are both 3×10^{-4} s^{-1}. This symmetry supports the assumption that the tidal plume is not significantly affected by the earth's rotation during its initial stages. The total volumetric transport in the surface layer is 3.6×10^{4} m^3 s^{-1}.

The propagation of the tidal plume away from the river mouth and later in the tidal cycle is observed on line B (Figs. 8, 9 and 10). Since the tidal plume is less than 3 m deep at its outer edge, the vessel's underway CTD is our most reliable measure of the location of the tidal plume front. In Fig. 8a the northern front of the tidal plume is marked by a transition from a salinity of 19 to 21 at 46.33° N over a distance of 200 m. Behind (south of) the front the surface salinity increases to 20 over 5 km and then decreases to a minimum of 14.5 at 46.23° N. The point of minimum salinity also corresponds to the maximum offshore velocity, coincident with the core of the most recent ebb pulse from the estuary.

The velocity signal associated with the tidal plume is not easily distinguished in the east-west velocity record after the initial ebb pulse. In transect B1, 8.9 h after the maximum ebb outflow, the tidal plume has already begun to turn anticyclonically and align with the re-circulating plume (Fig. 8c). However, the eastward flow of the re-circulating plume is significantly reduced near the surface in the region south of the tidal plume front indicating that the two are not fully aligned. The flow of the tidal plume is more obvious in the north velocity record. It is marked by a strong northward velocity, which reaches 0.45 m s^{-1} in the upper 5 m of the water column (Fig. 8d). The northward flow is intense near the front and propagates deeper into the water column. The velocity of the tidal plume can no longer be distinguished from the re-circulating plume 14.7 h after high tide (Fig. 10c and d).

Due to the momentum from the river, the tidal plume is a high energy feature and the site of elevated mixing. A fine-structure turbulent length-scale analysis similar to Orton and Jay (2005) enables us to estimate mixing parameters in regions of energetic mixing using CTD density data, and conservative “ceiling” or maximum possible values for regions of weak mixing. The eddy diffusivity for the core of the tidal plume as it crosses line B was 3.9×10^{-4} m^2 s^{-1} ($2.5–5.0\times10^{-4}$ bootstrapped 95% confidence interval). For comparison, the eddy diffusivity in the upper 14 m of the re-circulating flow north of 46.28° N was 1.5×10^{-5} m^2 s^{-1} (0.4×10^{-5}–2.5×10^{-5}), over an order of magnitude smaller than in the westward-moving core.

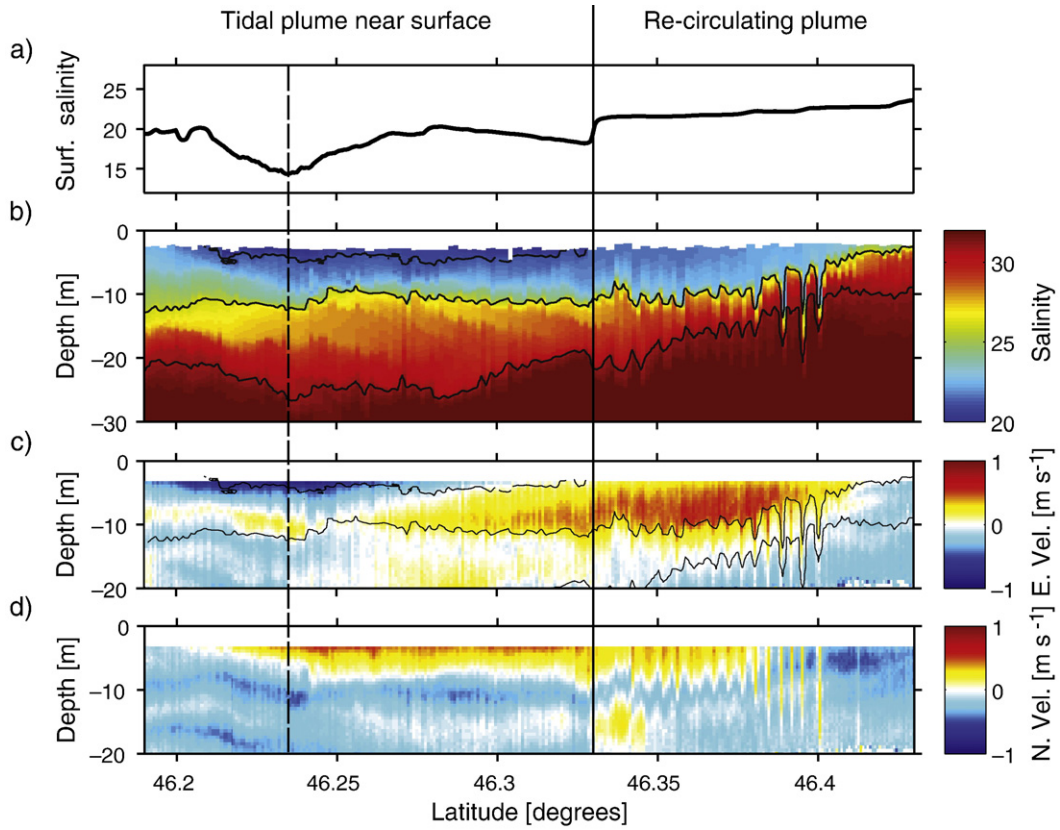

Fig. 8. Data from Line B1, 8.9 h after high tide on June 10, 2005. This transect intersects the anticyclonic circulation in the middle of the plume. a) Surface salinity indicates the location of the northern front of the tidal plume, but shows only a gradual increase toward the northern edge of the re-circulating plume. b) Salinity from the Triaxus towfish in the upper water column. The black contours are 21, 26 and 32 salinity isohalines, which approximately delineate the tidal, re-circulating and far-field plume water masses. c) and d) show East and North velocity, respectively. Salinity contours from b) are plotted on c) for comparison. The vertical solid line marks the northern front of the tidal plume, which divides the tidal and re-circulating plumes on the surface. The vertical dashed line marks the approximate axis of the estuary outflow.

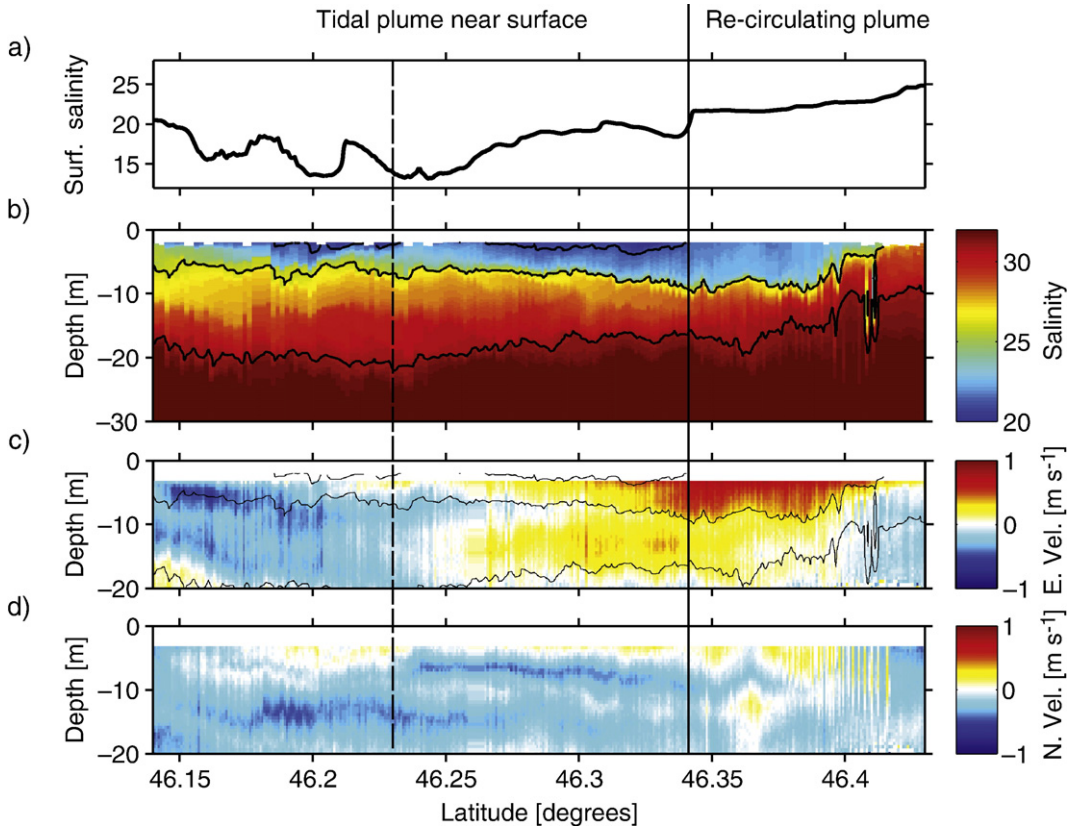

Fig. 9. Data from Line B2, 11.6 h after high tide on June 10, 2005. This transect intersects the anticyclonic circulation in the middle of the plume. See description of panels in Fig. 8 caption.

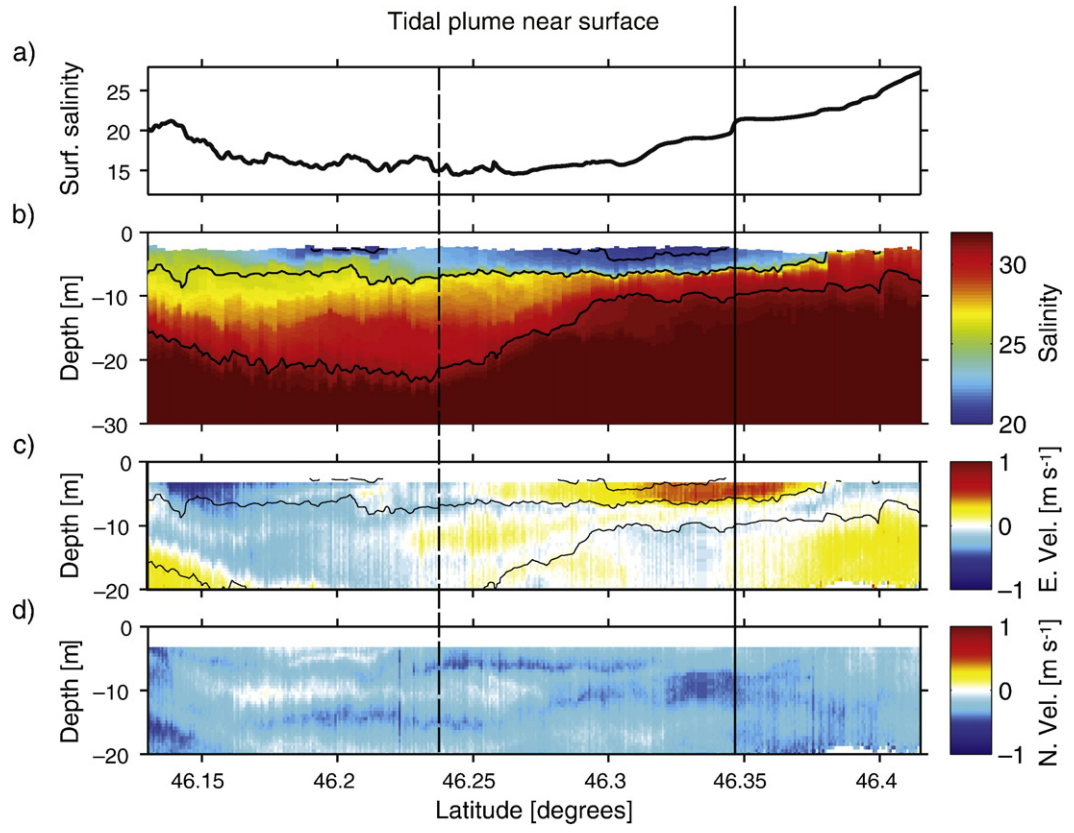

Fig. 10. Data from Line B3, 14.7 h after high tide on June 10, 2005. See description of panels in Fig. 8 caption.

4.3. Re-circulating plume

Sampling on Line B, which illustrates the properties of the re-circulating plume most clearly, started during the greater flood, 9.6 h after high tide (Fig. 8). Data from these transects document the persistent anticyclonic flow in the re-circulating plume and the northward propagation of the tidal plume over top of it. The re-circulating plume is 5 to 10 m deep and extends from beyond the southern end of Transect B to a wide front at the northern end. The average surface velocity is westward in the southern half of the transect and eastward in the northern half, consistent with the anticyclonic bulge circulation with a center of rotation approximately located at the latitude of the river mouth. The velocity increases away from the center of rotation to approximately 0.5 m s^{-1} at a distance of 10 km from the bulge center. This circulation persists throughout the 3 day sampling period on Line A and Line B (Fig. 10 a–f).

The re-circulating plume contains low-salinity water that is marked by higher velocities than the surrounding far-field plume. The northern front separating the re-circulating plume from the far-field plume is evident in the each of the first three passes between 46.33° N and 46.4°N (e.g. Figs. 8, 9 and 10). Defining the frontal region in this case as the region where the plume bottom slope is high, the front width varies between 3 and 5 km. In the same region the surface salinity increases monotonically from 20 to 28. The re-circulating plume front has negligible convergence, but it is marked by a consistent horizontal velocity shear. In Transect B1, the near-surface velocity varies from 0.6 m s^{-1} in the eastward jet to 0 m s^{-1} at the edge of the front over 5 km, corresponding to an average shear of 1.2×10^{-4} s^{-1}.

The observations of the re-circulating plume on Line B are analyzed in detail in Horner-Devine (2009). This work draws three conclusions that are significant to the present discussion. First, the structure of the re-circulating plume is consistent with the bulge observed in laboratory (Horner-Devine et al., 2006) and numerical models (Fong and Geyer, 2002). The existence of the bulge in river plumes has been the focus of considerable discussion and it has often been considered to be an artifact generated by the simplifications necessary for models (Garvine, 2001). The observations on Line B provide good evidence of the existence of the bulge circulation in the Columbia plume during periods of moderate or low wind stress. Second, the momentum within the re-circulating plume is observed to be in gradient-wind balance, as predicted in analytical models (Yankovsky and Chapman, 1997; Nof and Pichevin, 2001) and laboratory experiments (Horner-Devine et al., 2006). Thus, the dynamics of the re-circulating plume are distinct from the tidal plume, which is supercritical for much of its transit and strongly influenced by the momentum of the river discharge. Finally, the volume of freshwater in the re-circulating plume is greater than 3 days worth of river discharge. This confirms that the re-circulating plume retains a large fraction of water discharged from the estuary. The implications of the re-circulating plume as a large retentive coastal feature are discussed in more detail in Section 5.

4.4. Interaction of the tidal and re-circulating plumes

As discussed in Section 2.3, the dynamics of the tidal plume and re-circulating plume are expected to be strongly coupled. Mixing between the two occurs along the tidal plume front and due to internal waves emitted from the front as it slows. The density contrast between the tidal plume and the underlying water mass will affect the propagation speed and intensity of the front and internal waves. These dynamics are observed as the tidal plume passes over the re-circulating plume along Line B (Figs. 8–10).

At the time of the first pass (B1), the tide has been flooding at the estuary mouth for 3 h and thus the tidal plume is no longer forced by the momentum of the estuary outflow. The front propagation speed determined by comparing transects B1 and B2 is 0.23 m s^{-1}. This is well below the calculated intrinsic wave speed in the plume, confirming that the front has transitioned from a supercritical to a subcritical state. Propagation continues until 15–20 h after high tide (Fig. 11). At this point the location of the front stalls, suggesting that it loses energy as it approaches the northern boundary of the re-circulating plume (Fig. 11e and f). During this period, the surface salinity in the center of the transect, south of the tidal plume front, increases constantly from 15 on Transect B1 to 20–21 on Transect B5

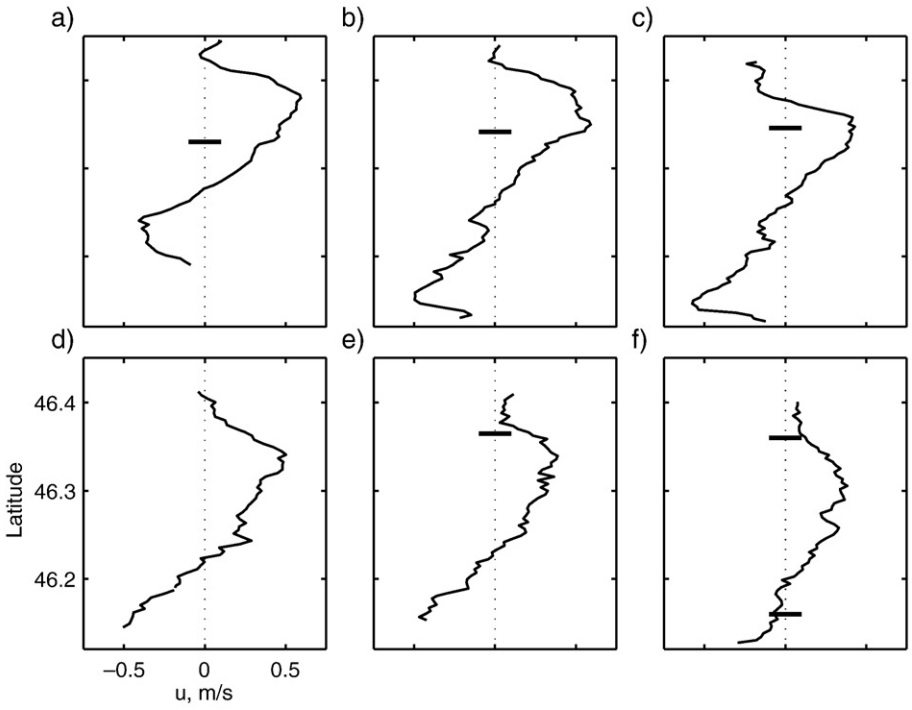

Fig. 11. East velocity in the upper 5 m of the water column on Line B. The short thick line indicates the location of the tidal plume front determined from the surface salinity (see Figs. 7, 8 and 9). Relative to the high tide before the greater ebb, the average time of each pass is a) 8.8, b) 11.6, c) 14.7, d) 19.8, e) 22.9, and f) 25.6 h.

(not shown). Mixing between the tidal and re-circulating plumes appears to have eroded the salinity anomaly in the tidal plume by this time.

The locations of the first three observations of the tidal plume front are also plotted on Fig. 2a. This SAR image shows the plume 1 h later than transect A1 relative to the phase of the tide, but 7 days earlier. The June 3 plume in the SAR image has propagated further north and has not yet released internal waves on the northern front. The tidal amplitude and river discharge were 5% and 15% higher, respectively, on June 3 compared with June 10. This suggests that the discharge may play a large role in setting the size of the tidal plume.

More than 10 solitons have been released by the front at the time of the first pass on Line B and they have propagated away from the front (Fig. 8). The solitons are clear in the velocity data; each trough is marked by elevated north and east velocity components. However, the TRIAXUS does not resolve the solitons well due to aliasing between the sampling frequency and the soliton wavelength. The soliton packet is observed again in Transect B2, 2.0 km north along the transect (Fig. 9). Front-normal velocities are estimated by determining the effective center for the radial spreading of the tidal plume from SAR images (e.g. Fig. 2a) and calculating the change in the position of the wave packet relative to that location. For the internal wave packet, the front-normal propagation speed is 0.69 m s^{-1}. For comparison, the observed density profile in the region of the re-circulating plume immediately north of the tidal plume front was used to calculate a first mode baroclinic wave speed of 0.63 m s^{-1}. As observed by Nash and Moum (2005), the measured propagation speed exceeds the intrinsic wave speed due to finite amplitude effects.

In the far-field region north of the re-circulating plume, the surface layer is considerably more saline. The intrinsic wave speed based on the observed density profile north of the re-circulating plume front is 0.33 m s^{-1}, approximately half the speed in the re-circulating plume. As a result, internal waves propagating from south to north will slow as they move through the re-circulating plume front. As the packet of internal waves impinges on the front of the re-circulating plume it distorts the front, forcing the interface down (Fig. 9). Although it is difficult to reliably estimate the mixing caused by this interaction, it is likely that the waves, which penetrate well below the interface, result in considerable vertical exchange between the re-circulating plume and the underlying higher-salinity water. In the subsequent transect, which crossed the frontal region 4.3 h later, there is little evidence of the internal waves, and the re-circulating plume has been reset (Fig. 10). Pan and Jay (2008) have shown that solitons are capable of transporting low-salinity fluid across the front due to a Stokes drift mechanism.

4.5. Upwelling conditions

The cross-shore Line C, which shows the westward motion of the plume, was sampled during upwelling conditions three days after sampling on Lines A and B. Observations from this line demonstrate the off-shore extent, right-ward turning and cross-frontal shear of the tidal plume as well as the overall plume structure during upwelling winds. The re-circulating plume flow appears to be attenuated by the upwelling wind stress, which opposes the flow at the outer edge of the plume. The tidal plume structure, however, remains clear.

The salinity structure of the westward-propagating tidal plume during the stronger ebb-flood phases on June 13–14 is shown in Fig. 12, and the surface salinity and velocity are shown in Fig. 13. Early in the ebb, the offshore edge of the new tidal plume extends to 124.23° W, but the front is weak. Offshore of the tidal plume, a 10 to 15 m thick layer of higher salinity plume water extends to the end of the transect

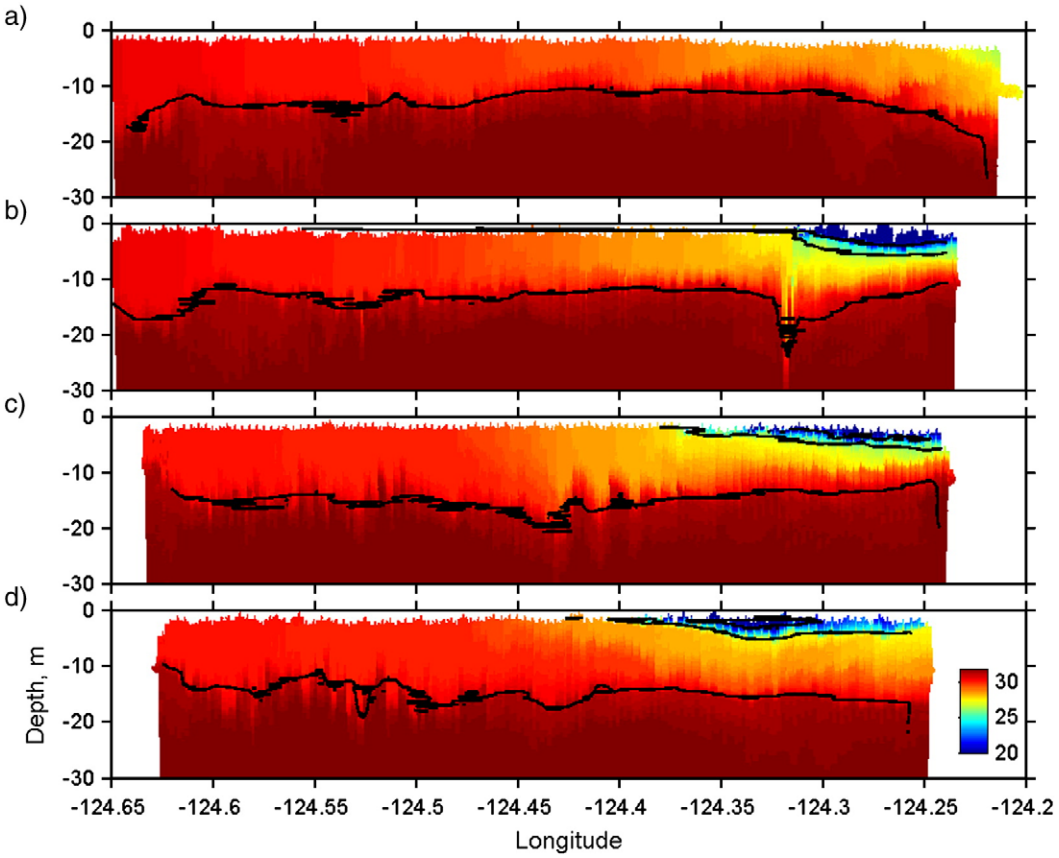

Fig. 12. Salinity from the Triaxus towfish in the upper water column from Lines C2–C5, 2.4–11.1 h after high tide, respectively, on June 13–14, 2005. The black lines are 21, 26 and 32 salinity isohalines, which approximately delineate the tidal, re-circulating and far-field plume water masses. a)–d) correspond to panels b)–e) in Fig. 10, where the tidal phase is indicated.

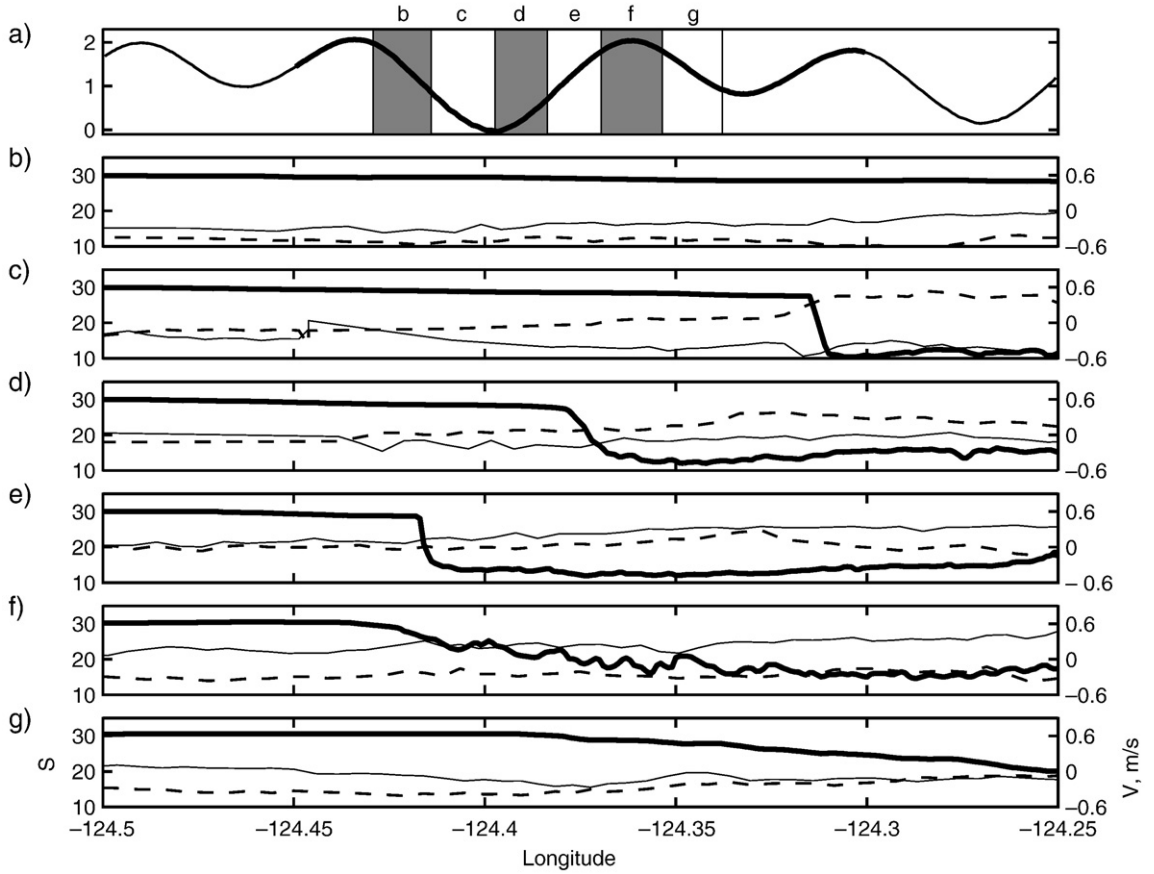

Fig. 13. Surface salinity (left axis) and velocity (right axis) record from the EW Line C on June 13–14, 2005. a) Tidal cycle showing the sampling period for each pass. The entire sampling period is shown with a darker line and alternate passes are shaded. b)–i) Surface salinity (thick line), and East (thin line) and North (dashed line) surface velocity for passes 2–7, respectively. Letters in panel a) show the period of the tidal cycle corresponding to each panel.

at 124.65° W. The salinity in this layer increases away from the coast, from approximately 28 near the new plume to 30 at the western end of the transect (Fig. 12a). The offshore velocity field is concentrated within this surface layer and oriented to the south and west, consistent with the upwelling surface stress (Fig. 13b).

As the ebb intensifies, a strong front forms at the western boundary of the tidal plume extending to more than 20 m depth, with a salinity change of 14.5 occurring over 200 m. The front was captured immediately after the first internal waves were released, 4.8 h after high tide and 20 km from the river mouth (Figs. 12b and 13c). Thus, the relaxation of the front and release of internal waves occurs soon after the ebb discharge peaks and the momentum forcing subsides. From this point on, the tidal plume has a Froude number below 1 (DJ) and propagation is driven primarily by the buoyancy of the new plume water. The near surface velocity field corresponding to the tidal plume is westward and northward (Fig. 13c). The northward front-parallel velocity is approximately 0.5 m s^{-1} and the jet is 5 km wide.

At the beginning of the flood, 8.4 h after high tide, the front has released a series of solitons and become less sharp (Fig. 12c and 13d). The tidal plume has thinned and now extends out to 124.38° W. The fission process and relaxation of this front is described in more detail in DJ and Nash and Moum (2005). The frontal jet is still strong, and has rotated anticyclonically towards due north. Later in flood, 11.1 h after high tide, the tidal plume front has progressed 8.5 km further west to 124.42° W and, according to the surface salinity record (Fig. 12e), has re-sharpened. Although the strong ebb discharge from the estuary has subsided at this point, the flood tide on the shelf now opposes the expansion of the tidal plume, which continues to propagate westward due to its own buoyancy and the residual discharge of freshwater from the estuary. This convergence appears to be sufficient to sharpen the front a second time. However, no deep-penetrating frontal structure is observed at the location of the flood surface front (not-shown). Twelve hours after high tide, the front is much more diffuse, with a lateral salinity gradient that extends across a 9 km frontal zone. This marks the furthest offshore penetration of the tidal plume, 28.5 km from the river mouth and the end of the tidal plume. For comparison, the outer limit of the tidal front on June 3, 2005 was at least 40 km from the mouth (Fig. 2a). The difference is likely due to greater tidal amplitude and higher river discharge earlier in the month.

In Figs. 12 and 13 and in the description above, the tidal plume is observed to propagate directly into a brackish far-field plume that is 10 to 15 m deep and extends beyond the western end of the transect (124.6° W). Thus, during strong upwelling winds, freshwater is carried away from the river mouth by Ekman transport and no persistent re-circulating plume forms. The extension of the proposed conceptual model to upwelling conditions is described in Fig. 3c and Section 5.3.

5. Discussion and implications

The Columbia plume is characteristic of large-scale mid-latitude plumes with respect to its sub-tidal circulation and response to atmospheric forcing, but also retains the intense fronts and strong tidal variability that are typically associated with smaller-scale plumes. The existence of these two flow regimes in the region offshore of the estuary mouth results in a complex and variable plume structure. The conceptual model described in Section 2 and Fig. 3 deconstructs this region of the plume into separate components in order to improve our understanding of the combined system. The observations focus on the interaction of the tidal and re-circulating

plumes, and note that a layer of higher salinity water, which is the far-field plume, is always observed around and beneath the more dynamic components of the re-circulating plume.

5.1. Interaction of offshore water masses

The interaction of the three offshore water masses that make up the plume is summarized in a cartoon in Fig. 14, which represents the flow along Line B shortly after the end of the greater ebb. The tidal plume, which we define as the pulse of low-salinity water discharged from the estuary during the ebb, flows over top of the older plume water on the shelf. During peak ebb it forms an intense westward current that is 3 to 5 m deep with surface velocities of 1 to 2 m s^{-1} 20 km from the mouth. At this point, the tidal plume is spreading radially away from the river mouth, but is beginning to tend north, consistent with an inertial radius of 20 to 30 km for the maximum ebb current. At the end of the ebb, the tidal plume thins and slows, and the front speed drops below the ambient wave speed and releases solitons. By this time, the outer region of the tidal plume has also acquired a significant northward velocity due to Coriolis acceleration.

The re-circulating plume receives momentum and buoyancy from the tidal plume and, during the low-wind period, persists for several days offshore and slightly north of the river mouth. The total volume of freshwater in this region of the plume is equivalent to approximately 3 to 4 days of river discharge, indicating that the residence time is on that order. Based on the north-south transects, the anticyclonic circulation is approximately 20 km across, with maximum east and west velocities of 0.5 m s^{-1}.

While the three offshore plume water masses are described in terms of their time scales and horizontal extents, they can also be thought of in terms of different salinity classes. In this regard, the plumes can also be differentiated vertically. The re-circulating plume flows within the saltier far-field plume, and the tidal plume flows over top of the re-circulating plume. Buoyancy is transferred from the tidal plume downward (and outward) to the re-circulating plume by buoyancy flux arising from mixing at the interface and the tidal plume front.

Mixing between the re-circulating plume and tidal plume results from interfacial shear at the base of the tidal plume and the front (e.g. Fig. 9). It was noted in Section 2 that the tidal plume front is typically stronger on the north than the south, and that internal waves are released earlier on the south. This observation is in part explained by the vorticity imparted in the tidal plume by the tidal flow (DJ). It may also be explained by the relative velocities of the tidal and re-circulating plumes. During peak ebb, when the tidal plume is initiated, it travels westward and spreads radially away from the mouth (Fig. 6e) over top of the re-circulating plume. In this region, directly offshore of the estuary mouth, the tidal plume and re-circulating plume velocities are aligned. However, the re-circulating plume velocity opposes that of the early tidal plume to the north. Thus, the frontal Froude number is expected to be higher on the north side of the plume than the south. The additional shear due to the re-circulating plume may contribute to the north-south asymmetry described in DJ, and may help to explain the observed pattern of internal waves in Fig. 2a.

5.2. Downwelling winds

The conceptual model presented herein extends naturally to include the effects of wind stress, which is often of major importance in determining the plume dynamics. In the presence of strong, persistent downwelling winds, Ekman transport moves the re-circulating and far-field plumes shoreward; the plume is pressed against the coast and transport of plume water away from the mouth to the north increases (Fig. 3b). If the wind stress is sufficiently strong, it augments the alongshore flux of plume water such that all of the estuary discharge is transported northward within one inertial period, resulting in little accumulation of buoyant fluid in the re-circulating plume region. Within the downwelling plume, brackish water tends to be well-mixed vertically. The coastal water, therefore, consists of a band of brackish water close to the coast and high-salinity water immediately offshore, neither of which is strongly stratified. Under these conditions, the tidal plume can propagate offshore beyond the existing plume water into unstratified shelf water. Consequently, the density contrast between the tidal plume water and the receiving water is low in the near-shore band and high offshore of the downwelled plume. As the tidal plume propagates beyond the downwelling front, the present conceptual model predicts that the high density contrast will inhibit mixing between the tidal plume and the water below it and result in a tidal plume front that propagates rapidly outwards. Due to the lack of stratification in the receiving water, energy cannot be released from the out-flowing tidal plume by means of internal waves and soliton generation is not usually observed. While strong, persistent downwelling winds are not common during spring and summer, they are a frequent winter pattern. In summer, downwelling conditions typically follow upwelling and carry old plume water back to the coast. This results in a more stratified and more complex sets of dynamics than those described by the present conceptual model.

5.3. Upwelling winds

In the presence of strong persistent upwelling winds, the Columbia plume is directed southward and offshore (Hickey et al., 2005). In this case, plume water is transported away from the river mouth due to offshore Ekman transport and mixed to form an extensive stratified plume (Figs. 3c and 12). As with the downwelling case, sufficient wind stress will transport plume water away from the mouth at a rate

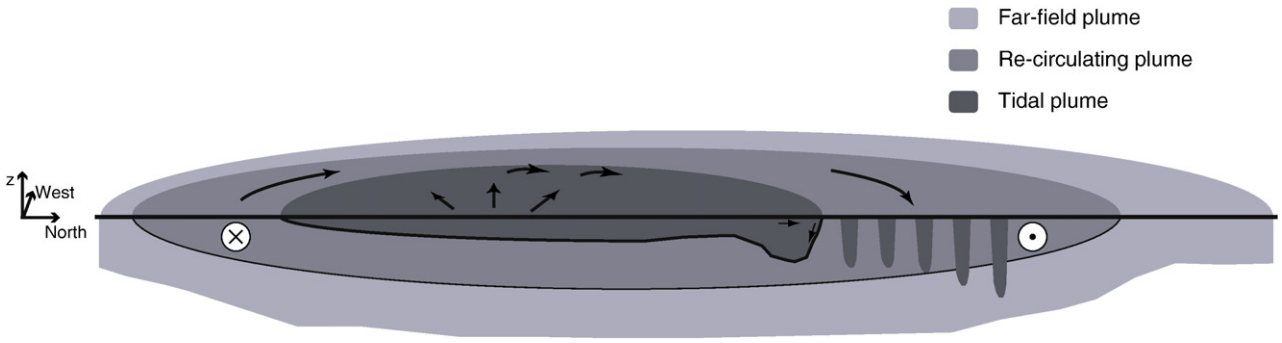

Fig. 14. Cartoon showing the interaction between the three plume water masses from above and from the side under light wind conditions. The re-circulating plume flows in an anticyclonic direction within the far-field plume. The tidal plume initially propagates west, spreading north and south. As it approaches its westward extent, the tidal plume is deflected increasingly to the north.

similar to the estuary discharge and no accumulation of water will occur in the re-circulating plume. However, since much of the upwelled water is transported offshore, the effective width of the plume is very large. Consequently, the tidal plume propagates offshore into a broad stratified plume far-field. In contrast to the downwelling case, the density contrast between the tidal plume and the receiving water is lower, resulting in a lower propagation speed for the tidal plume and more mixing between the two. Also, stratification in the receiving water supports internal waves and the outward propagating front loses energy as solitons are generated and propagate away from the tidal plume (Fig. 12b and c). There is an important exception to this description. Since the upwelling plume is directed offshore and southwards, the northern boundary of the existing plume may be close to shore, forcing the tidal plume to propagate into salty unstratified ocean water on its northwestern edge. Very strong fronts are often observed under these conditions, due presumably to the combination of the high density contrast and convergent flow from the north. This situation appears to be quite favorable for mixing upwelled nutrients into the plume.

5.4. Chemical and ecological implications

The dynamics of the source, tidal, re-circulating and far-field plumes may have important implications for the coastal ecosystem. Freshwater has different residence times in the four water masses, and moves sequentially from one water mass to the next. Thus, the four environments represent different stages in biological growth. In particular, phytoplankton typical of the plume environment have doubling rates in this region on the order of a day (Landry et al., 1989), and are expected to have different signatures in the tidal, re-circulating and far-field plumes.

The re-circulating plume can loosely be referred to as an "estuary at sea", because the waters are brackish and, due to its bounding front and circulation, residence times are relatively long. Chlorophyll concentrations are low in the estuary and source zone, because of low light and nutrient levels and residence times (Small and Prahl, 2004). Over 90% of the estuary, including embayments and tidal marshes, has a water residence time below 1 day (Bottom et al., 2005). The source zone and tidal plume are characterized by time scales of 2 h and 0.5 days, respectively; these are also short relative to the doubling time of phytoplankton cells and allow for little growth. On the other hand, the residence time in the re-circulating plume is observed to be 3 to 4 days, providing a favorable environment for growth.

This contrast is apparent in the record of surface chlorophyll concentration during the occupation of line A. The surface chlorophyll a concentration (chl a), which was calibrated using in situ samples ($R^2 = 0.94$; J. Peterson pers. comm.), varies consistently between the three water masses on line A; however, it does not vary monotonically with salinity (Fig. 6a). In Fig. 15a chl a is plotted against surface salinity for the 36 h occupation of Line A. The high salinity water in the far field plume has relatively low chl a (4–7 mg m^{-3}) compared with the inflowing tidal plume (6–9 mg m^{-3}). The highest concentration, however, is observed in the re-circulating plume (8–14 mg m^{-3}). Enhanced mixing (reported herein) and nutrient entrainment (Lohan and Bruland, 2006) between the tidal plume and underlying water masses causes each pulse to become enriched as it propagates out to sea and eventually melds into the re-circulating plume. While these observations over-simplify a complex biological system, they suggest that the tidally-pulsed nutrient delivery, increased residence time of brackish water, and the shallow plume depth all contribute to a higher phytoplankton biomass in the re-circulating plume.

The same trend is observed initially along Line B. Low salinity water within the tidal plume front is associated with lower chl a concentrations, and higher salinity water in the re-circulating plume with higher concentrations (Fig. 15b,c and d). The distinction between tidal and re-circulating plumes persists until approximately 18 h after the peak ebb (Transect B4, Fig. 15e). At this point the trend reverses, resulting in surface plume water south of the tidal plume front with higher chl a than water north of the front. This trend suggests that, through a combination of mixing with existing plume water and/or growth of phytoplankton within the plume, chl a increases above the level of the older plume water. In our final pass on Line B, we see the process repeating itself. The subsequent tidal plume carries new fresh water across the existing plume with lower chl a concentration (Fig. 15g).

6. Summary

We have presented a conceptual model of the Columbia River plume that differentiates between four plume water masses: the plume source region, and the tidal, re-circulating and far-field plumes. This classification describes distinct stages of mixing from the lowest salinity estuary water to the final mixing of plume water in the far-field plume. Low salinity estuary water is initially mixed with coastal waters in the source region, which is within the mouth of the estuary. During ebb tide, a tidal plume forms and propagates out across the shelf in a shallow, energetic layer. The tidal plume is initially bounded

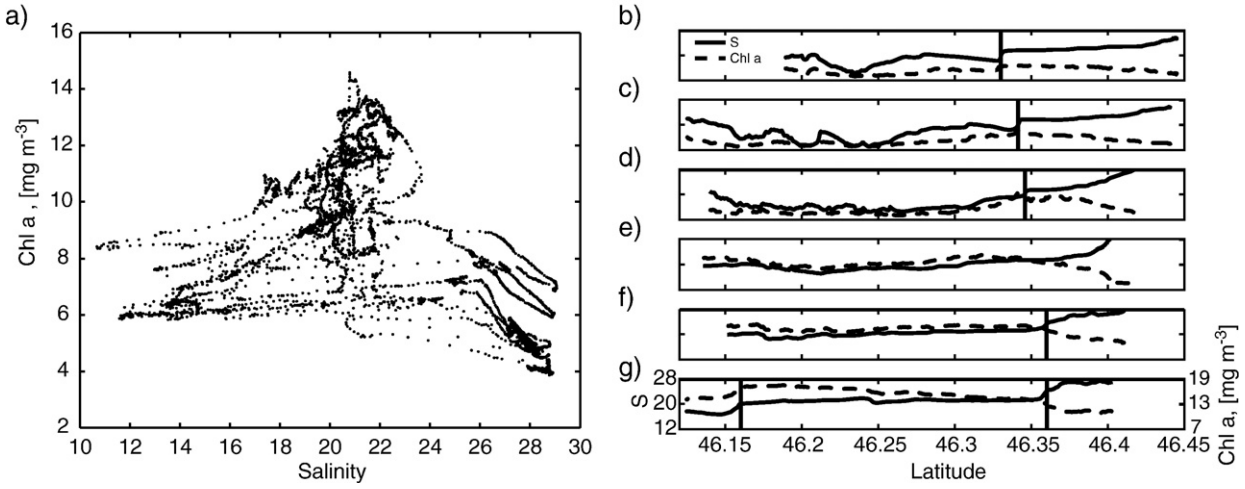

Fig. 15. a) Surface chlorophyll a concentration vs. surface salinity for all transects on Line A. High salinity water (far-field plume) is associated with the lowest chlorophyll concentrations, low salinity water (tidal plume) is associated with slightly higher concentrations and intermediate salinity water (re-circulating plume) has the highest chlorophyll concentration. b–g) Surface salinity and chlorophyll a concentration from all transects on Line B.

by strong, convergent fronts. As the ebb subsides, the tidal plume loses energy and the front spawns solitons. The tidal plume continues to propagate outward across the shelf until approximately 12 h after high tide, when it loses its coherence and melds into the existing plume circulation. During periods of low wind stress, the subtidal plume circulation consists of a persistent anticyclonic circulation resembling the bulge circulation observed in laboratory and numerical model studies.

The tidal plume over-runs the re-circulating plume, contributing momentum and buoyancy. Solitons released from the tidal plume front penetrate well below the lower interface of the re-circulating plume and mix it with the underlying high salinity water. They are observed to distort and deepen the re-circulating plume front as they impinge upon it. The out-flowing tidal plume is initially aligned with the flow of the re-circulating plume on the south end, but not on the north. This misalignment may contribute relatively more vertical shear to the north and may explain why internal waves are generated earlier on the south side of the plume and fronts are stronger to the north.

Finally, we observe consistent variation in the chlorophyll concentration in the three offshore plume water masses. During the low-wind sampling period, the surface chlorophyll concentration was lowest in the far-field plume, higher in the tidal plume and highest in the re-circulating plume. This suggests that these water masses, which are differentiated in terms of their residence times, also correspond to distinct biological growth zones.

The observations from June 8 to 10 support the conceptual model of the plume structure during periods of low wind. During a subsequent period of upwelling wind, this structure is observed to be modified significantly; the retentive re-circulating plume circulation has all but disappeared. Analyses that predict wind conditions (both magnitude and persistence) and differentiate between these modes of plume behavior are needed to understand how nutrients, organisms and other water-borne scalars are retained and transported in the plume.

Acknowledgments

The authors would like to thank Raphael Kudela and Jiayi Pan for making satellite images available, and Jay Peterson and Keith Leffler for help on the cruises. This research was funded by the Bonneville Power Administration and NOAA-Fisheries (project: Ocean Survival of Salmonids), University of Washington Royalty Research Fund, and the National Science Foundation (project RISE – River Influences on Shelf Ecosystems OCE 0239072 and OCE 0648655). We also thank Captain Ron L. Short of the R/V Pt Sur and Marine Technicians Stewart Lamberdin, Christina Courcier, and Ben Jokinen for their superb support of in-situ data collection. The SAR images were provided by Comprehensive Large Array-data Stewardship System (CLASS) of National Oceanic and Atmospheric Administration (NOAA). This is RISE contribution number 9.

References

Barnes, C., Duxbury, A., Morse, B., 1972. Circulation and selected properties of the Columbia River effluent at sea. In: Pruter, A., Alverson, D. (Eds.), The Columbia River Estuary and Adjacent Ocean Waters. University of Washington Press, Seattle, WA, pp. 41–80.

Bottom, D.L., Simenstad, C.A., Burke, J., Baptista, A.M., Jay, A.D., Jones, K.K., Casillas, E., Schiewe, M.H., 2005. Salmon at river's end: the role of the estuary in the decline and recovery of Columbia River salmon. U.S. Dept. of Commerce, NOAA Tech. Memo., NMFS-NWFSC-68, 246 p (final report).

Chao, S.Y., 1990. Tidal modulation of estuarine plumes. Journal of Physical Oceanography 20 (7), 1115–1123.

Cudaback, C.N., Jay, D.A., 2000. Tidal asymmetry in an estuarine pycnocline: depth and thickness. Journal of Geophysical Research-Oceans 105 (C11), 26,237–26,251.

Fong, D.A., Geyer, W.R., 2002. The alongshore transport of fresh water in a surface-trapped river plume. Journal of Physical Oceanography 32 (3), 957–972.

Garcia-Berdeal, I., Hickey, B., Kawase, M., 2002. Influence of wind stress and ambient flow on a high discharge river plume. Journal of Geophysical Research 107, (C9).

Garvine, R.W., 1974. Dynamics of small-scale oceanic fronts. Journal of Physical Oceanography 4 (4), 557–569.

Garvine, R.W., 1979a. Integral hydrodynamic model of upper ocean frontal dynamics. 1. Development and analysis. Journal of Physical Oceanography 9 (1), 1–18.

Garvine, R.W., 1979b. Integral hydrodynamic model of upper ocean frontal dynamics. 2. Physical characteristics and comparison with observations. Journal of Physical Oceanography 9 (1), 19–36.

Garvine, R.W., 1982. A steady state model for buoyant surface plume hydrodynamics in coastal waters. Tellus 34, 293–306.

Garvine, R.W., 1995. A dynamical system for classifying buoyant coastal discharges. Contintental Shelf Research 15 (13), 1585–1596.

Garvine, R.W., 2001. The impact of model configuration in studies of buoyant coastal discharge. Journal of Marine Research 59, 193–225.

Garvine, R.W., Monk, J.D., 1974. Frontal structure of a river plume. Journal of Geophysical Research 79 (15), 2251–2259.

Hessner, K., Rubino, A., Brandt, P., Alpers, W., 2001. The rhine outflow plume studied by the analysis of synthetic aperture radar data and numerical simulations. Journal of Physical Oceanography 31 (10), 3030–3044.

Hetland, R., 2005. Relating river plume structure to vertical mixing. Journal of Physical Oceanography 35 (9), 1667–1688.

Hickey, B.M., Peitrafesa, L.J., Jay, D.A., Boicourt, W.C., 1998. The Columbia River plume study: subtidal variability in the velocity and salinity field. Journal of Geophysical Research 103 (C5), 10,339–10,368.

Hickey, B., Geier, S., Kachel, N., MacFadyen, A.F., 2005. A bi-directional river plume: the Columbia in summer. Continental Shelf Research 25 (14), 1631–1656.

Horner-Devine, A.R., 2009. The bulge circulation in the Columbia River plume. Continental Shelf Research 29, 234–251. doi:10.1016/j.csr.2007.12.012.

Horner-Devine, A.R., Fong, D.A., Monismith, S.G., Maxworthy, T., 2006. Laboratory experiments simulating a coastal river inflow. Journal of Fluid Mechanics 555, 203–232.

Jay, D., Pan, J., Orton, P., Horner-Devine, A., (this volume) Asymmetry of tidal plume fronts in an eastern boundary current regime. Journal of Marine Systems.

Landry, M., Postel, J., Peterson, W., Newman, J., 1989. Broad-scale distributional patterns of hydrographic variables on the Washington/Oregon shelf. In: Landry, M., Hickey, B.M. (Eds.), Coastal Oceanography of Washington and Oregon. Elsevier, Amsterdam, pp. 1–40.

Lohan, M., Bruland, K., 2006. Importance of vertical mixing for additional sources of nitrate and iron to surface waters of the Columbia River plume: implications for biology. Marine Chemistry 98, 260–273.

MacDonald, D.G., Geyer, W.R., 2004. Turbulent energy production and entrainment at a highly stratified estuarine front. Journal of Geophysical Research-Oceans 109, (C5).

Nash, J.D., Moum, J.N., 2005. River plumes as a source of large-amplitude internal waves in the coastal ocean. Nature 437 (7057), 400–403.

Nof, D., Pichevin, T., 2001. The ballooning of outflows. Journal of Physical Oceanography 31 (10), 3045–3058.

O'Donnell, J., Marmorino, G.O., Trump, C.L., 1998. Convergence and downwelling at a river plume front. Journal of Physical Oceanography 28 (7), 1481–1495.

Orton, P.M., Jay, D.A., 2005. Observations at the tidal plume front of a high-volume river outflow. Geophysical Research Letters 32 (11).

Pan, J., Jay, D., 2008. Dynamic characteristics and horizontal transports of internal solitons generated at the Columbia River plume front. Continental Shelf Research. doi:10.1016/j.csr.2008.01.002.

Pritchard, M., Huntley, D.A., 2006. A simplified energy and mixing budget for a small river plume discharge. Journal of Geophysical Research-Oceans 111 (C3).

Small, L.F., Prahl, F.G., 2004. A particle conveyor belt process in the Columbia River estuary: evidence from chlorophyll a and particulate organic carbon. Estuaries 27 (6), 999–1013.

Yankovsky, A.E., Chapman, D.C., 1997. A simple theory for the fate of buoyant coastal discharges. Journal of Physical Oceanography 27 (7), 1386–1401.

Yankovsky, A.E., Hickey, B.M., Munchow, A.K., 2001. Impact of variable inflow on the dynamics of a coastal buoyant plume. Journal of Geophysical Research-Oceans 106 (C9), 19,809–19,824.

Zimmerman, J.T.F., 1981. Dynamics, diffusion and geomorphological significance of tidal residual eddies. Nature 290 (5807), 549–555.